Anderson lattice in the intermediate valence compound $Ce_3Ni_2B_2N_{3-\delta}$

Tahir Ali, Ernst Bauer, Gerfried Hilscher, and Herwig Michor*
Institut für Festkörperphysik, Technische Universität Wien, A-1040 Wien, Austria
(Received 12 August 2010; revised manuscript received 8 February 2011; published 21 March 2011)

We have studied magnetic, thermodynamic, and transport properties of $Ce_3Ni_2B_2N_{3-\delta}$ and its solid solution with the $T_c \simeq 13$ K superconductor $La_3Ni_2B_2N_{3-\delta}$. The solid solution $(La,Ce)_3Ni_2B_2N_{3-\delta}$ reveals a rapid reduction of T_c by increasing the Ce content with a complete suppression of superconductivity at the composition $La_{2.85}Ce_{0.15}Ni_2B_2N_{3-\delta}$. The low-temperature properties characterize $Ce_3Ni_2B_2N_{3-\delta}$ as an intermediate valence system with a moderately enhanced Sommerfeld value $\gamma \simeq 54$ mJ/mol K^2 and a susceptibility $\chi_0 \simeq 1.6 \times 10^{-3}$ emu/mol, increased by about one order of magnitude as compared to the respective value $\chi_0 \simeq 0.2 \times 10^{-3}$ emu/mol of superconducting $La_3Ni_2B_2N_{3-\delta}$ ($\gamma = 26$ mJ/mol K^2) which serves as reference with a nonmagnetic rare earth ion. The electrical resistivity and thermoelectric power of $Ce_3Ni_2B_2N_{3-\delta}$ are analyzed in terms of the degenerate Anderson lattice model revealing a characteristic Kondo temperature $T_K^{\mathrm{ALM}} \sim 1100$ K.

DOI: 10.1103/PhysRevB.83.115131 PACS number(s): 65.40.Ba, 72.15.Qm, 74.70.Dd, 75.20.Hr

I. INTRODUCTION

The persistent interest in intermetallic compounds containing cerium is due to their rich low-temperature physics interrelated with ground states such as the Kondo lattice with and without long-range magnetic order, intermediate valence, Kondo insulator, and in some cases unconventional superconductivity (see, e.g., Ref. 1 for a recent review). This variety of ground states adopted in cerium compounds is a consequence of competing interactions: RKKY-type Ce-Ce intersite exchange, crystal field effects, and Kondo interaction between Ce $4f$ and conduction electrons. A subtle balance between RKKY and Kondo interactions in some cases leads to the formation of novel ground states of correlated electrons such as magnetically mediated unconventional superconductivity. Cerium based superconductors at ambient pressure are, e.g., $CeCu_2Si_2$, $CeTIn_5$, and non-centrosymmetric $CePt_3Si$.[2–4] From the earliest studies of magnetic pair breaking effects in rare earth elements by Matthias *et al.*[5] cerium has been known to act as a strongly pair breaking impurity in a superconducting matrix.

A prominent system among intermetallics showing interplay of magnetism and superconductivity is the quaternary borocarbide, RNi_2B_2C (R = rare earths and Y), with relatively high T_c (up to 16 K; see, e.g., Refs. 6 and 7). In the corresponding solid solution with cerium, $Y_{1-x}Ce_xNi_2B_2C$, a complete suppression of superconductivity was observed at $x \geqslant 0.25$.[8] Studies of structural and magnetic features of $CeNi_2B_2C$ revealed intermediate valence of Ce and absence of superconductivity down to 2 K.[9,10] Interestingly, El-Massalami *et al.*[11] reported conventional BCS type superconductivity for $CeNi_2B_2C$ at temperatures below $T_c \simeq 100$ mK. The related quaternary boronitride, $La_3Ni_2B_2N_{3-\delta}$, with rocksalt type triple LaN layer sheets in between the NiB layers shows superconductivity with $T_c \sim 12$–15 K.[12–14] A cerium based homologue, $Ce_3Ni_2B_2N_{3-\delta}$, was synthesized as powder material via a metathesis reaction by Glaser *et al.*[16] Magnetic susceptibility measurements down to 5 K revealed neither superconductivity nor magnetic ordering.[16]

In this paper we investigate the ground state properties of bulk metallic samples of $(La,Ce)_3Ni_2B_2N_{3-\delta}$ by means of x-ray diffraction, susceptibility, specific heat, and transport measurements.

II. EXPERIMENTAL DETAILS

Polycrystalline samples of $(La,Ce)_3Ni_2B_2N_{3-\delta}$ were prepared by inductive levitation melting in a three step process. In the first step, stoichiometric amounts of Ni and B were melted several times in Ar atmosphere. In a second step, La and Ce metals were premelted in vacuum and then melted with NiB forming $(La,Ce)_3Ni_2B_2$ precursor alloys. In a third step these alloys were repeatedly melted in Ar/N_2 atmosphere such that the N-stoichiometry is slowly increased to reach a composition close to a nominal stoichiometry $(La,Ce)_3Ni_2B_2N_{\sim 2.7}$. The latter was determined by measuring the mass gain after each melting cycle and by measuring the pressure drop within the recipient. The $(La,Ce)_3Ni_2B_2N_{3-\delta}$ alloys were flipped after each melting cycle to improve their homogeneity. The samples were finally annealed in a high-vacuum furnace at 1100 °C for 1 week. The starting materials were La and Ce ingot (Metall Rare Earth, 99.9%), Ni (Alpha Aesar, 99.99%), crystalline boron (HCTS, 99.5%), and nitrogen gas (Linde, 99.999 %). An additional $Ce_3Ni_2B_2N_{\sim 2.7}$ sample has been prepared using high purity Ce ingot (Ames MPC,[17] 99.95%). The nominal stoichiometry $(La,Ce)_3Ni_2B_2N_{\sim 2.7}$ was chosen because it was found to give the highest phase purity.

The phase purity of the samples was checked by powder x-ray diffraction (XRD) on a Siemens D5000 diffractometer using monochromated Cu Kα radiation. Full profile Rietveld refinements were carried out using the FULLPROF program.[18] Magnetic measurements were performed on a CRYOGENIC SQUID magnetometer (3 K to room temperature) and on a Quantum Design 9 T vibrating sample magnetometer (VMS) equipped with a VSM oven operating up to 1000 K. Resistivity measurements were carried out on bar shaped samples with a standard four probe method in a ^{4}He cryostat (4 – 400 K) and for $Ce_3Ni_2B_2N_{3-\delta}$ additionally in a ^{3}He cryostat down to 350 mK. Specific heat measurements were made on 2–3 g samples employing an adiabatic step heating technique. Measurements of the thermoelectric power (TEP) were carried out from 4 K to 300 K with a so-called differential

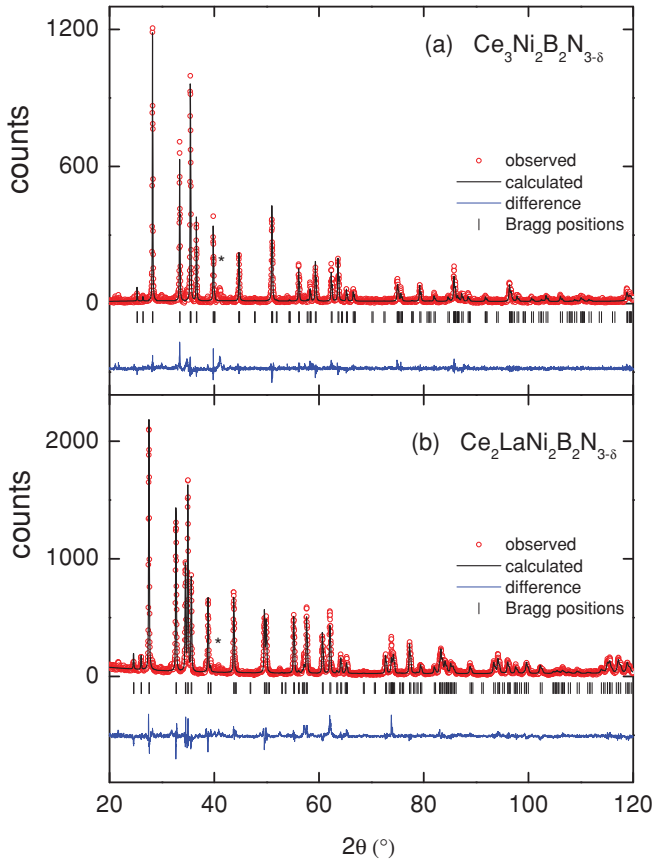

FIG. 1. (Color online) Measured room-temperature XRD pattern of $LaCe_2Ni_2B_2N_{3-\delta}$ and $Ce_3Ni_2B_2N_{3-\delta}$. The solid lines derive from the Rietveld refinements. The strongest impurity line is marked by an asterisk.

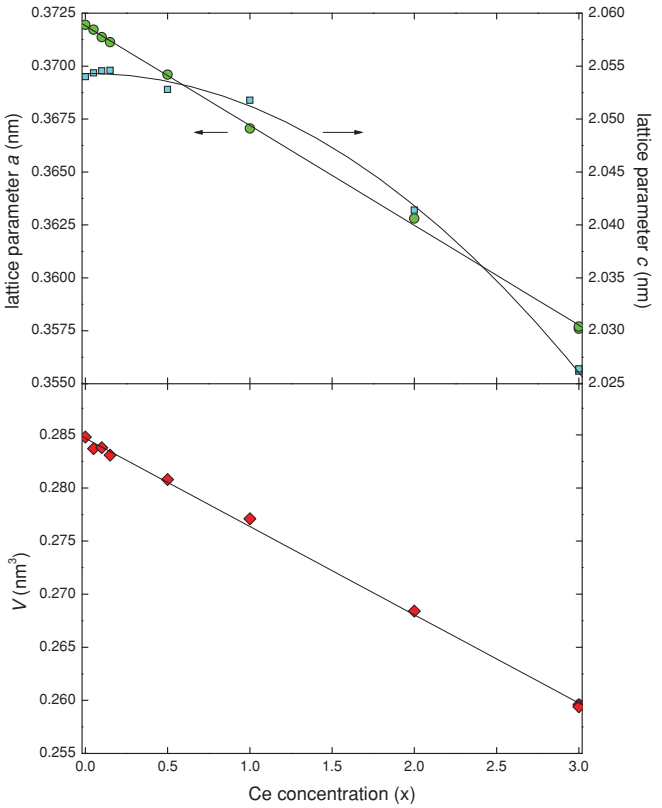

FIG. 2. (Color online) Variation of the lattice parameters a (circles) and c (squares) (top panel) and unit cell volume (bottom panel) in the solid solution $La_{3-x}Ce_xNi_2B_2N_{3-\delta}$; lines are guides to the eye.

seesaw heating method in a ^{4}He cryostat and high-temperature measurements (340–800 K) were carried out on an ULVAC ZEM-3 measuring system.

III. RESULTS AND DISCUSSION

A. Structural characterization

Powder XRD data of all samples of the series $La_{3-x}Ce_xNi_2B_2N_{3-\delta}$ display the body centered tetragonal $La_3Ni_2B_2N_3$ type structure with space group $I4/mmm$. Except for $Ce_3Ni_2B_2N_{3-\delta}$, some minor admixtures of the related two-layer boronitride (La,Ce)NiBN are identified with phase fractions of up to 5%. In the case of $Ce_3Ni_2B_2N_{3-\delta}$ traces of an unidentified impurity phase are observed for both samples, one prepared with cerium produced by Metall Rare Earth and one prepared with highest purity cerium prepared by Ames MPC, but the two-layer phase CeNiBN is not observed. Two exemplary powder XRD patterns of $La_{3-x}Ce_xNi_2B_2N_{3-\delta}$ and their Rietveld refinements are shown in Fig. 1.

The variation of the lattice parameters a and c in the solid solution $La_{3-x}Ce_xNi_2B_2N_{3-\delta}$ is summarized in Fig. 2. The lattice parameters a and c obtained for $Ce_3Ni_2B_2N_{3-\delta}$ are 0.357 nm and 2.025 nm, respectively. These values are in good agreement with the lattice parameters reported earlier.[16] The reduction of the unit cell volume of $Ce_3Ni_2B_2N_{3-\delta}$ as compared to $La_3Ni_2B_2N_{3-\delta}$ is about 9%. As expected from the lanthanide contraction, the a lattice parameter decreases with increasing Ce fraction; however, the c lattice parameter shows a nonmonotonic variation with a maximum at about $x = 0.2$. An even opposite trend for the variation of the a and c lattice parameters was reported for the related quaternary borocarbides[9] which has been attributed to rather stiff Ni-B and B-C bonds leading to an increase in B-Ni-B tetrahedral angle and thus to a stretching of the tetragonal c axis when the basal plane lattice constant a contracts. The lanthanide contraction in $La_{3-x}Ce_xNi_2B_2N_{3-\delta}$ causes a similar effect on the NiB layers and their tetrahedral bonding angle which changes from ~106° for $La_3Ni_2B_2N_{3-\delta}$ to ~104° for $Ce_3Ni_2B_2N_{3-\delta}$, however, in this case with an additional change in the width (parallel to the c axis) of the (La,Ce)N triple layers, thus causing the nonmonotonic variation of the c lattice parameter shown in Fig. 2. We note that the change of the unit cell volume by about 9% in the series $(La,Ce)_3Ni_2B_2N_{3-\delta}$ is two orders of magnitude larger than the volume changes caused by varying the nominal nitrogen stoichiometry in $La_3Ni_2B_2N_x$.[14]

B. Superconductivity in $La_{3-x}Ce_xNi_2B_2N_{3-\delta}$

The superconducting transition temperatures of $La_{3-x}Ce_xNi_2B_2N_{3-\delta}$ with $x = 0$, 0.05, and 0.1 were determined from dc susceptibility measurements (see Fig. 3) which were performed after zero field cooling (ZFC) at a field of 1 mT. Field-cooled susceptibility (not shown for the sake of clarity in Fig. 3) reveal Meissner fractions

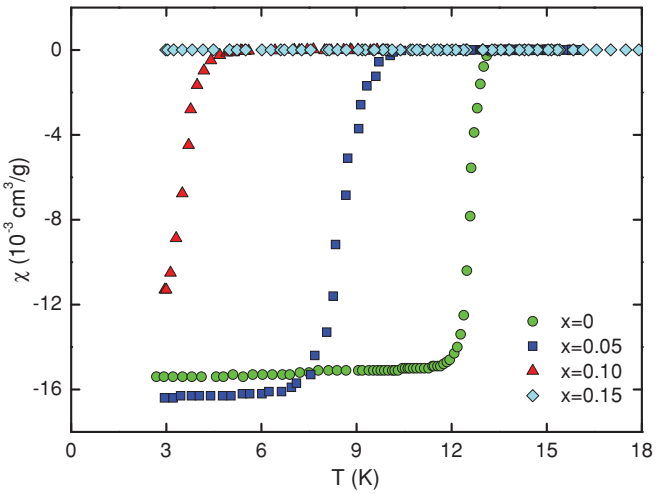

FIG. 3. (Color online) Temperature-dependent susceptibility for $La_{3-x}Ce_xNi_2B_2N_{3-\delta}$ measured at 1 mT (ZFC) with x as labeled.

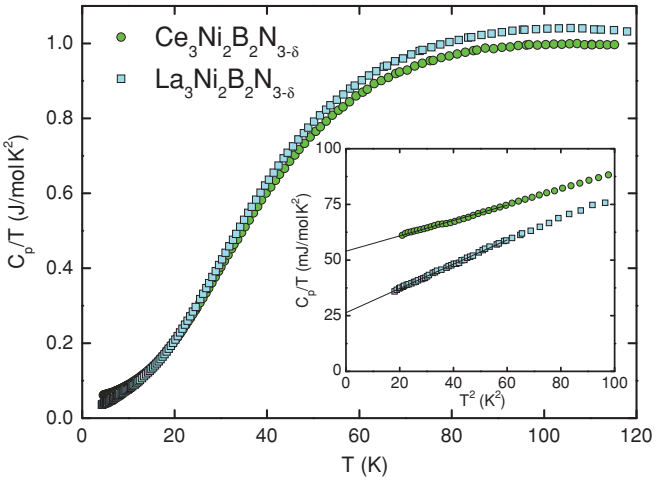

FIG. 4. (Color online) Specific heat of $Ce_3Ni_2B_2N_{3-\delta}$ (0 T) and $La_3Ni_2B_2N_{3-\delta}$ (9 T) at selected temperatures. Inset: C/T vs T^2 graph of the low-temperature part with solid lines indicating $C/T = \gamma + \beta T^2$ linear fits.

of about 10% due to strong pinning effects. The latter was discussed in detail in Ref. 19. The susceptibility data reveal an almost linear reduction of T_c with increasing Ce fraction at a rate of $dT_c/dx \simeq -8.9$ K/Ce% in the formula $La_3Ni_2B_2N_{3-\delta}$ and a corresponding critical concentration for the suppression of superconductivity of 1.3% Ce in the full formula with 10 atoms. In related light rare earth solid solutions $La_{3-x}R_xNi_2B_2N_{3-\delta}$ with R = Pr and Nd we observed one order of magnitude larger critical concentrations of 19% and 10%, respectively.[15] The more rapid suppression of T_c in $La_{3-x}Ce_xNi_2B_2N_{3-\delta}$, i.e., the stronger pair-breaking introduced by Ce ions, is attributed to Kondo interactions and valence fluctuations. Interestingly, although parent boronitride and borocarbide compounds, $La_3Ni_2B_2N_{3-\delta}$ and YNi_2B_2C, exhibit similar values of $T_c \simeq 13$ and 15 K, and similar upper critical fields $H_{c2}(0) \sim 5 - 8$ T,[20] the rate of suppression of T_c by Ce subsitution in the boronitride system is significantly larger than the corresponding value of -2.5 K/Ce% reported by Alleno *et al.*[8] for the related borocarbide system $Y_{1-x}Ce_xNi_2B_2C$.

C. Ground state properties of $Ce_3Ni_2B_2N_{3-\delta}$

1. Results of thermodynamic and transport studies

The ground state properties of $Ce_3Ni_2B_2N_{3-\delta}$ were studied by means of specific heat, magnetic susceptibility, resistivity, and thermoelectric power measurements. The normal state properties of $La_3Ni_2B_2N_{3-\delta}$ with an empty $4f$ shell are used as a reference for non-$4f$ contributions. The specific heat of $Ce_3Ni_2B_2N_{3-\delta}$ measured at zero external field and the normal state specific heat of $La_3Ni_2B_2N_{3-\delta}$ measured at 9 T are shown in Fig. 4 as C_p/T vs T. The low-temperature electronic and lattice contributions of a plain metal are given by $C_p = C_e + C_{\rm ph} \simeq \gamma + \beta T^3$ where γ is the Sommerfeld value and β is related to the low-temperature Debye temperature $\Theta_D^{\rm LT} = (1944 \times n/\beta)^{1/3}$, where $n = 10$ is number of atoms per formula unit. From the low-temperature fit of the $Ce_3Ni_2B_2N_{3-\delta}$ data (see inset in Fig. 4) we obtain $\gamma \simeq 54$ mJ/mol K^2 and $\beta \simeq 0.36$ mJ/mol K^4 corresponding to $\Theta_D^{\rm LT} = 378$ K. The latter, however, might be misleading because the $C \propto \beta T^3$ lattice term is superimposed by magnetic contributions from Ce $4f$ orbitals. In the case of $La_3Ni_2B_2N_{3-\delta}$ the low-temperature data yield $\gamma \simeq 26$ mJ/mol K^2 and $\Theta_D^{\rm LT} \simeq 329$ K which are in agreement with the values reported in Ref. 19, $\gamma \simeq 26$ mJ/mol K^2 and $\Theta_D^{\rm LT} \simeq 303$ K. The enhanced electronic contribution to the specific heat of $Ce_3Ni_2B_2N_{3-\delta}$ as compared to $La_3Ni_2B_2N_{3-\delta}$, i.e., $\Delta\gamma \simeq 28$ mJ/K^{2}mol, is attributed to magnetic contributions of Ce-$4f$ in the intermediate valent regime.

The dc magnetic susceptibilities of $Ce_3Ni_2B_2N_{3-\delta}$ and $La_3Ni_2B_2N_{3-\delta}$ were measured from 3 K to room temperature (RT) and from RT to 1000 K at applied fields of 1 T and 9 T, respectively [see Fig. 5 (a)]. While $La_3Ni_2B_2N_{3-\delta}$ displays (above its T_c) a simple, weakly temperature dependent Pauli paramagnetism with a low-temperature susceptibility, $\chi_0 \simeq 0.2 \times 10^{-3}$ emu/mol, $Ce_3Ni_2B_2N_{3-\delta}$ exhibits about an order of magnitude larger susceptibility with a maximum at about 800 K. For both compounds, a small additional Curie-Weiss component is observed at low temperatures and a corresponding fit of the data from 10 to 200 K in terms of a temperature-independent component χ_0 plus a Curie-Weiss term $\chi = \chi_0 + C/(T - \theta)$ where C the Curie constant and θ the paramagnetic Curie temperature yielding for $Ce_3Ni_2B_2N_{3-\delta}$ a $\chi_0 \simeq 1.6 \times 10^{-3}$ emu/mol and $C \simeq 9 \times 10^{-3}$ emu K/mol. In the case of $La_3Ni_2B_2N_{\sim 3}$ the fit of the low-temperature magnetic susceptibility data gives $\chi_0 \simeq 0.2 \times 10^{-3}$ emu/mol and $C \simeq 4 \times 10^{-3}$ emu K/mol. The paramagnetic Curie temperature for both the samples is of the order of -10 K. The Curie-Weiss-like contribution in $Ce_3Ni_2B_2N_{3-\delta}$ is attributed to paramagnetic impurities (e.g., Gd traces of the order of 100 ppm in the La and Ce raw elements) and seems to be not an intrinsic property. The values of χ_0 and C obtained for $La_3Ni_2B_2N_{3-\delta}$ are close to values reported earlier.[21]

The moderately temperature dependent but nevertheless largely enhanced susceptibility of $Ce_3Ni_2B_2N_{3-\delta}$ is attributed to f-electron contributions from intermediate valent Ce ions with strongly Kondo screened Ce $4f$ moments. In

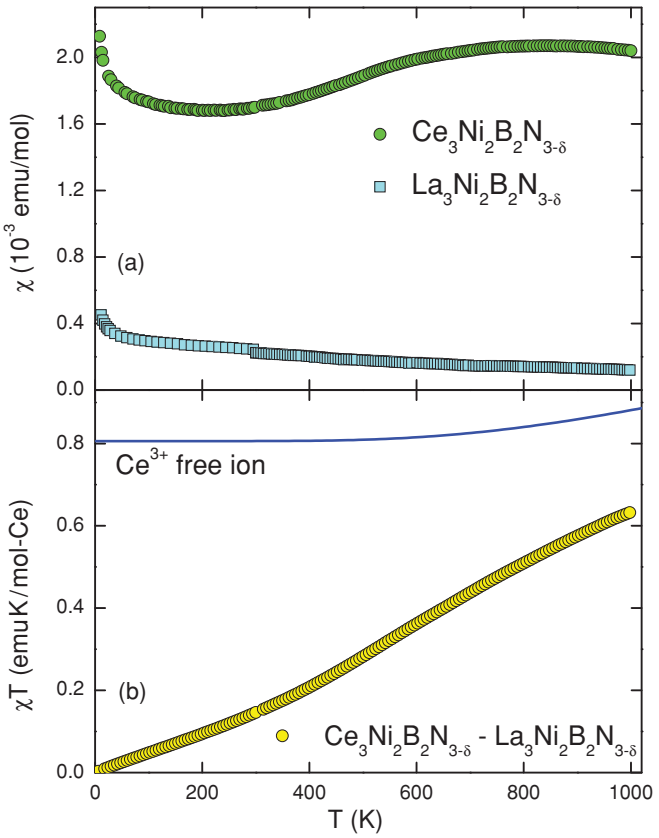

FIG. 5. (Color online) Temperature-dependent susceptibility of $Ce_3Ni_2B_2N_{3-\delta}$ and $La_3Ni_2B_2N_{3-\delta}$ measured at applied fields of 1 T below 300 K and at 9 T above (a). Product of the Ce-4f magnetic susceptibility with temperature χT vs temperature (b). The solid line indicates the theoretical χT of free Ce^{3+} ions.

order to obtain a measure for the $4f$ occupation from the susceptibility data we follow the approach proposed in Refs. 22–24. Comparison of the $Ce_3Ni_2B_2N_{3-\delta}$ $4f$ susceptibility (obtained by subtracting the $La_3Ni_2B_2N_{3-\delta}$ data) with the theoretical susceptibility of Ce^{3+} ions ($4f^1$ configuration with a ground state total angular momentum $J = 5/2$ and excited state $J = 7/2$ separated by a spin-orbit splitting $\Delta \simeq 3150$ K; see, e.g., Ref. 26) in a χT versus T plot in Fig. 5 (b) suggests a $4f$ occupation clearly larger than 0.7. We note that the temperature-dependent susceptibility $\chi(T)$ of $Ce_3Ni_2B_2N_{3-\delta}$ in Fig. 5(a) compares rather well with, e.g., $\chi(T)$ of $CeIr_2$ showing just slightly lower absolute values as compared to $Ce_3Ni_2B_2N_{3-\delta}$ and a weak maximum at a slightly higher temperature ~1000 K.[23] The values of χT(1000 K) are 0.63 emu K/mol-Ce and ~0.55 emu K/mol-Ce for $Ce_3Ni_2B_2N_{3-\delta}$ and $CeIr_2$, respectively. For $CeIr_2$ a cerium valence of 3.2 –3.23 has been reported from L_{III} x-ray absorption studies.[24,25] Thus, a realistic estimate for the $4f$ occupation of $Ce_3Ni_2B_2N_{3-\delta}$ is near 0.8.

The $4f$ contribution to the low-temperature susceptibility $\Delta\chi(0) \simeq 1.4 \times 10^{-3}$ emu/mol and the Sommerfeld value $\Delta\gamma \simeq 28$ mJ/K^{2}mol is analyzed in terms of the Fermi-liquid relation (see, e.g., Ref. 27),

$$R g_J^2 J(J+1)\mu_B^2 \Delta\gamma = \pi^2 k_B^2 \Delta\chi, \qquad (1)$$

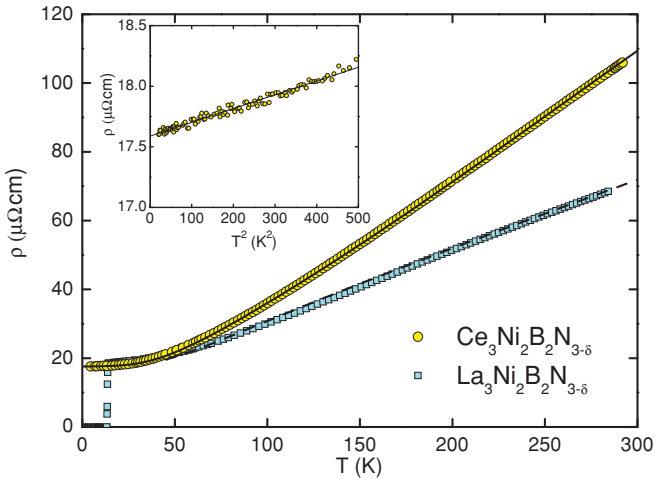

FIG. 6. (Color online) The electrical resistivity $\rho(T)$ of $Ce_3Ni_2B_2N_{3-\delta}$ and $La_3Ni_2B_2N_{3-\delta}$. The solid line indicates a fit according to the ALM and the dashed line shows the normal metal $\rho_0 + \rho_{BG}$ contribution included in this fit. Inset: ρ vs T^2 graph of the $Ce_3Ni_2B_2N_{3-\delta}$ data.

yielding for $J = 5/2$ an experimental value of the Wilson ratio $R \simeq 1.8$ being slightly larger than the value expected for a degenerate $Ce^{\sim 3.2+}$ state,[28,29] $R = N/[N - 1 + (n_f - 1)^2] \simeq 1.19$ for a degeneracy $N = 6$ and $n_f \simeq 0.8$.

The temperature-dependent electrical resistivity $\rho(T)$ of $La_3Ni_2B_2N_{3-\delta}$ and $Ce_3Ni_2B_2N_{3-\delta}$ is shown in Fig. 6. Except for small variations of the residual resistivities, absolute values of $\rho(T)$ obtained in this study have been well reproduced with several samples of $La_3Ni_2B_2N_{3-\delta}$[14] and $Ce_3Ni_2B_2N_{3-\delta}$. The superconducting $La_3Ni_2B_2N_{3-\delta}$ has a $T_c^\rho \simeq 12.5$ K while $Ce_3Ni_2B_2N_{3-\delta}$ remains in the normal state at least down to the base temperature of the experiment, i.e., 0.35 K. At temperatures below 30 K, the $\rho(T)$ vs T^2 graph of the experimental data shown as an inset in Fig. 3 reveals a quadratic temperature dependence $\rho(T) = \rho_0 + AT^2$, with $A \simeq 1.2 \times 10^{-9}$ Ω cm/K^2. This coefficient A yields a Kadowaki-Woods ratio $A/\gamma^2 \simeq 4 \times 10^{-6}\mu\Omega$ cm (K mol-Ce/mJ)^2 which is in between the typical Kadowaki-Woods ratio $A/\gamma^2 \sim 10^{-5}\,\mu\Omega$ cm (K mol-Ce/mJ)^2 of (mostly twofold degenerate) cerium Kondo-lattice systems and the expected generalized Kadowaki-Woods ratio of Kondo lattice systems with sixfold degenerate Ce-4f moments[30] yielding $A/\gamma^2 \sim 0.7 \times 10^{-6}\,\mu\Omega$ cm (mol K/mJ)^2.

The value of the coefficient A together with the Sommerfeld coefficient of the electronic specific heat is indicative of Kondo interaction in $Ce_3Ni_2B_2N_{3-\delta}$ with a relatively high Kondo temperature as compared to typical crystal field splittings of the $J = 5/2$ multiplet of the Ce $4f^1$ state. Accordingly, numerical results of a sixfold degenerate Anderson lattice model (ALM) without Ce-Ce intersite coupling compiled by Cox and Grewe[31] are used to analyze the resistivity and thermoelectric power [ALM model provides $S(T > 0.2T_K^{ALM})$; see below] of $Ce_3Ni_2B_2N_{3-\delta}$. In the simple fully degenerate case, i.e., for strong Kondo coupling as compared to the crystal field splitting, the ALM yields a universal temperature dependency for the magnetic contribution to the resistivity and also the TEP, which simply scale with the Kondo temperature T_K^{ALM}.

To analyze the temperature-dependent resistivity data of $Ce_3Ni_2B_2N_{3-\delta}$ a magnetic contribution according to the numerical ALM results, $\rho_{\rm ALM}(T/T_K^{\rm ALM})$, is combined with a Bloch-Grüneisen (BG) model for the normal metal phonon contribution yielding

$$\rho(T) = \rho_0 + \alpha\,\rho_{\rm ALM}\left(T/T_K^{\rm ALM}\right) + \frac{4B}{\Theta_D}\left(\frac{T}{\Theta_D}\right)^5 \int_0^{\Theta_D/T} \frac{z^5 dz}{(e^z-1)(1-e^{-z})}. \qquad (2)$$

A reasonable set of parameters (further corroborated by the analysis of the thermoelectric power discussed below) is $\rho_0 = 17.6\ \mu\Omega$ cm [essentially fixed by $\rho(T \to 0)$ data], $\alpha = 89.6\ \mu\Omega$ cm, $T_K^{\rm ALM} = 1100$ K (characteristic Kondo temperature of the ALM model), the electron-phonon coupling constant $B = 0.013\ \Omega$ cm K, and Debye temperature $\Theta_D^{\rho} = 262$ K of the Bloch-Grüneisen model. The resulting fit is indicated as solid line in Fig. 6. The resulting normal metal contribution, i.e., residual resistivity ρ_0 plus phonon contribution according to the Bloch-Grüneisen fit, is in remarkably close agreement with the resistivity data of $La_3Ni_2B_2N_{3-\delta}$ (in absolute values). The characteristic energy scale $T_K^{\rm ALM} = 1100$ K is in fair agreement with the magnitude indicated by the maximum in the susceptibility near 800 K.

The temperature-dependent thermopower $S(T)$ of $La_3Ni_2B_2N_{3-\delta}$ and $Ce_3Ni_2B_2N_{3-\delta}$ is shown in Fig. 7(b). For $La_3Ni_2B_2N_{3-\delta}$, $S(T)$ is negative above T_c indicating a positive slope of the electronic density of states near the Fermi level. The mismatch between $T < 300$ K and $T > 300$ K data is an artifact of having used two different measuring techniques with imperfect overlap. The dashed-dotted line in Fig. 7(b) indicates a linear high-temperature extrapolation of the $T < 300$ K measurement corresponding to $S(T) = a + bT$ with $a = -16.7$ nV/K and $b = -1.77\ \mu$V/K^2.

The TEP for $Ce_3Ni_2B_2N_{3-\delta}$ exhibits a sharp linear increase at low temperature with an initial slope $S/T \simeq 0.2\ \mu$V/K and a broad Kondo maximum at high temperature with $S_{\rm max} \simeq 26\mu$V/K at about 500 K. The latter is analyzed in terms of the ALM data by Cox and Grewe[31] using the characteristic Kondo temperature $T_K = 1100$ K derived above. When comparing the TEP of $Ce_3Ni_2B_2N_{3-\delta}$ with the *clean limit* ALM calculation for sixfold degenerate $Ce^{\sim 3+}$ which yields a broad maximum $S_{\rm max} = 103\ \mu$V/K at $T/T_K \simeq 0.6$ (see Fig. 3 of Ref. 31), it is necessary to consider in addition to Kondo scattering, at least, also defect and phonon scattering. The summation of different contributions to the TEP is highly nontrivial, in particular for a quaternary, layered compound such as $Ce_3Ni_2B_2N_{3-\delta}$ with a complex multiband Fermi surface where in addition to contributions due to different scattering mechanisms, also contributions of different bands (index j) are to be added via the relation $S = \sum_j S^j\sigma^j/\sigma$ with σ^j being the electrical conductivity of band j (see, e.g., Ref. 32). The consideration of specific bands, however, looses relevance at elevated temperatures where interband scattering becomes strong. Thus, at high enough temperatures an estimate for the total diffusion thermopower S due to different types of scattering mechanisms α, e.g., electron-defect ($S_{e,0}$), electron-electron ($S_{e,e}$ or in the case of $Ce_3Ni_2B_2N_{3-\delta}$ the Kondo contribution $S_{\rm ALM}$ according to the ALM), and electron-phonon ($S_{\rm ep}$) scattering, is obtained via the Kohler relation,[33]

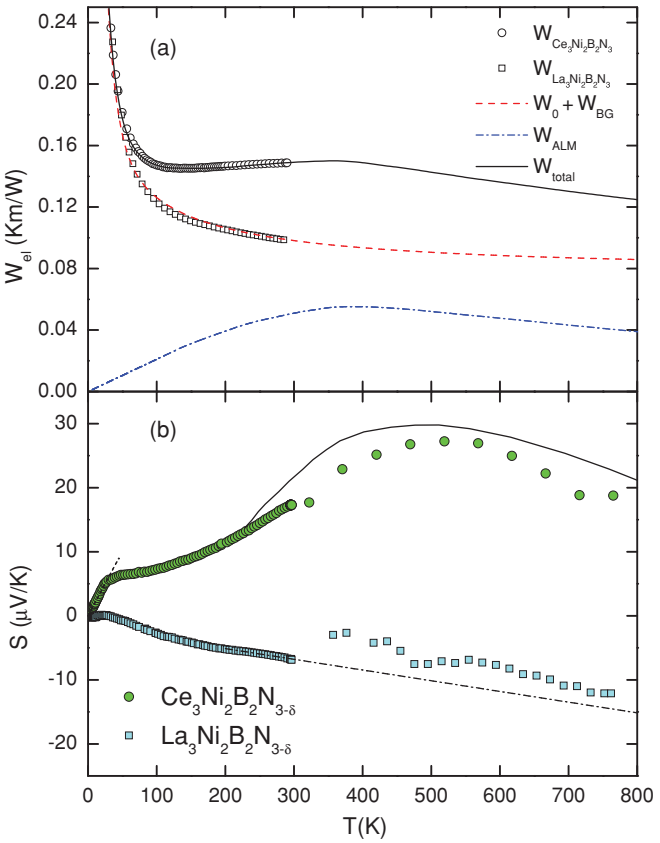

FIG. 7. (Color online) The electronic thermal resistance contributions estimated via the Wiedeman-Franz law from the electrical resistivity data and fitting by Eq. (2) (a). Temperature-dependent thermopower of $Ce_3Ni_2B_2N_{3-\delta}$ and $La_3Ni_2B_2N_{3-\delta}$ (b). The solid line indicates the ALM fit (see text); dashed and dash-dotted lines are straight lines.

$$S = W^{-1}\sum_\alpha S_\alpha W_\alpha, \qquad (3)$$

with W being the electronic thermal resistance. The latter obeys the Matthiessen rule, $W = \sum_\alpha W_\alpha$, where W_α are the contributions due to particular scattering mechanisms α. For simplicity of the analysis, W_α is estimated via the Wiedeman-Franz law, $W_\alpha(T) = \rho_\alpha(T)/L_\alpha T$, assuming $L_{e,0} \approx L_{\rm ep} \approx L_{e,e} \approx L_0 = 2.44 \times 10^{-8}\ {\rm W\Omega/K^2}$ (L_0 is the Lorenz-number) where Eq. (3) conforms to the Northeim-Gorter rule. Accordingly, contributions $W_{\rm ALM}$, $W_0 + W_{\rm BG}$, and the total electronic thermal resistance $W_{\rm total}$ corresponding to the above analysis of the resistivity data are displayed in Fig. 7(a). An estimate for the contribution $S_{e,0} + S_{\rm ep}$ is obtained from the $La_3Ni_2B_2N_{3-\delta}$ reference data [see the dashed-dotted line in Fig. 7(b)]. The latter together with the Kondo contribution $S_{\rm ALM}$ are added according to the Kohler relation, thus yielding a total TEP based on the degenerate ALM with $T_K = 1100$ K as indicated by the solid line in Fig. 7(b), which is in reasonable agreement with the experimental data.

The Kohler relation is not applicable in the low-temperature limit where many strongly correlated electron systems exhibit an approximately linear temperature dependence of the TEP which hardly depends on the level of elastic defect scattering

(corresponding to the residual resistivity ρ_0). Rather, the Seebeck coefficient S is related to the Sommerfeld coefficient γ,

$$\frac{S}{T} = q\frac{\gamma}{N_A e}, \tag{4}$$

where N_A is Avogadro's number and q is a dimensionless quantity which is found to be close to unity for most of the Ce based compounds.[34] For $\gamma \simeq 18$ mJ/K^{2}mol-Ce, the slope of the low-temperature part of the thermopower of $Ce_3Ni_2B_2N_{3-\delta}$ [dashed line in Fig. 7(b)] yields $S/T \simeq 0.2\ \mu$V/K^2 revealing $q \simeq 1$, well in line with the empirical trend observed for a large number of Ce based compounds compiled by Behnia *et al.* in Ref. 34. It is important to note that the T-linear TEP, and thus the phenomenological relation, Eq. (4), conforms with the Boltzmann picture of the free electron gas (see, e.g., Ref. 34), as well as with *clean limit ALM* results (see, e.g., Ref. 31). The prominent shoulder-like feature of $S(T)$ of $Ce_3Ni_2B_2N_{3-\delta}$ visible in Fig. 7(b) at about 20–150 K, thus, results from a crossover between the $S \propto \gamma T$ low-temperature regime and the high-temperature regime where different types of scattering mechanisms contribute to the the total diffusion thermopower as conceived by the Kohler relation. Accordingly, the shoulder-like feature of $S(T)$ does not relate to an energy scale of Kondo or valence fluctuations which should have an appropriate correspondence in specific heat and suceptibility data.

D. CONCLUSIONS

Powder XRD confirms the existence of a solid solution $La_{3-x}Ce_xNi_2B_2N_{3-\delta}$ from $x = 0 - 3$ with the $La_3Ni_2B_2N_3$ type structure and space group $I4/mmm$ whereby the lattice parameter a follows the lanthanide contraction, i.e., decreases with increasing Ce-fraction, but the lattice parameter c shows a nonmonotonic variation with a maximum at low Ce fraction ($x \sim 0.2$). With respect to superconductivity of the parent compound $La_3Ni_2B_2N_{3-\delta}$, which is observed below $T_c \simeq 13$ K in the present study, magnetic susceptibility data reveal a rapid reduction of T_c by increasing Ce content with a complete suppression of superconductivity at the composition $La_{2.85}Ce_{0.15}Ni_2B_2N_{3-\delta}$. The results of low-temperature magnetic, thermodynamic, and transport studies characterize $Ce_3Ni_2B_2N_{3-\delta}$ as an intermediate valence system with a Sommerfeld value $\gamma \simeq 54$ mJ/mol K^2 and a low-temperature susceptibility $\chi_0 \simeq 1.6 \times 10^{-3}$ emu/mol. The latter values are moderately enhanced with respect to the corresponding values of $La_3Ni_2B_2N_{3-\delta}$ with $\gamma = 26$ mJ/mol K^2 and $\chi_0 \simeq 0.2 \times 10^{-3}$ emu/mol. The high-temperature susceptibility indicates a Ce valence of about 3.2. The electrical resistivity and thermoelectric power are analyzed in terms of the degenerate Anderson lattice model revealing a Kondo temperature of $T_K^{\mathrm{ALM}} \sim 1100$ K.

*michor@ifp.tuwien.ac.at

[1] J. Sereni, in *Handbook on the Physics and Chemistry of Rare Earths*, edited by J. K. A. Gschneidner and L. Eyring (Elsevier, Amsterdam, 1991), Vol. 15, pp. 1–59.

[2] F. Steglich, J. Aarts, C. D. Bredl, W. Lieke, D. Meschede, W. Franz, and H. Schäfer, Phys. Rev. Lett. **43**, 1892 (1979).

[3] H. Hegger, C. Petrovic, E. G. Moshopoulou, M. F. Hundley, J. L. Sarrao, Z. Fisk, and J. D. Thompson, Phys. Rev. Lett. **84**, 4986 (2000).

[4] E. Bauer, G. Hilscher, H. Michor, C. Paul, E. W. Scheidt, A. Gribanov, Y. Seropegin, H. Noël, M. Sigrist, and P. Rogl, Phys. Rev. Lett. **92**, 027003 (2004).

[5] B. T. Matthias, H. Suhl, and E. Corenzwit, Phys. Rev. Lett. **1**, 92 (1958).

[6] K.-H. Müller and V. N. Narozhnyi, Rep. Prog. Phys. **64**, 943 (2001).

[7] L. C. Gupta, Adv. Phys. **55**, 691 (2006).

[8] E. Alleno, Z. Hossain, C. Godart, R. Nagarajan, and L. C. Gupta, Phys. Rev. B **52**, 7428 (1995).

[9] T. Siegrist, R. J. Cava, J. J. Krajewski, and W. F. J. Peck, J. Alloys Compd. **216**, 135 (1994).

[10] S. A. Carter, B. Batlogg, R. J. Cava, J. J. Krajewski, and W. F. Peck, Phys. Rev. B **51**, 12829 (1995).

[11] M. El Massalami, R. E. Rapp, and G. J. Nieuwenhuys, Physica C **304**, 184 (1998).

[12] R. J. Cava, H. W. Zandbergen, B. Batlogg, H. Eisaki, H. Takagi, J. J. Krajewski, W. F. Peck, E. M. Gyorgy, S. Uchida *et al.*, Nature (London) **372**, 245 (1994).

[13] H. W. Zandbergen, J. Jansen, R. J. Cava, J. J. Krajewski, and W. F. Peck, Nature (London) **372**, 759 (1994).

[14] T. Ali, C. Rupprecht, R. T. Khan, E. Bauer, G. Hilscher, and H. Michor, J. Phys. Conf. Ser. **200**, 012004 (2010).

[15] T. Ali, E. Bauer, G. Hilscher, and H. Michor, Solid State Phenomena e-print arXiv:1103.2947 (to be published 2011).

[16] J. Glaser, T. Mori, and H. Meyer, Z. Anorg. Allg. Chem. **634**, 1067 (2008).

[17] See [http://www.mpc.ameslab.gov].

[18] T. Roisnel and J. Rodriguez-Carvajal, Mater. Sci. Forum **378**, 118 (2001).

[19] H. Michor, R. Krendelsberger, G. Hilscher, E. Bauer, C. Dusek, R. Hauser, L. Naber, D. Werner, P. Rogl, and H. W. Zandbergen, Phys. Rev. B **54**, 9408 (1996).

[20] G. Hilscher and H. Michor, in *Studies on High Temperature Superconductors*, edited by A. Narlikar (Nova Science Publishers, New York, 1999), Vol. 28, pp. 241–285.

[21] H. Michor, G. Hilscher, R. Krendelsberger, P. Rogl, and F. Bourée, Phys. Rev. B **58**, 15045 (1998).

[22] B. C. Sales and D. Wohlleben, Phys. Rev. Lett. **35**, 1240 (1975).

[23] P. Weidner, B. Wittershagen, B. Roden, and D. Wohlleben, Solid State Commun. **58**, 915 (1983).

[24] D. Wohlleben, and J. Röhler, J. Appl. Phys. **55**, 1904 (1984).

[25] J. Röhler, in *Handbook on the Physics and Chemistry of Rare Earths*, edited by J. K. A. Gschneidner, L. Eyring, and S. Hüfner (Elsevier, Amsterdam, 1987), Vol. 10, pp. 453–545.

[26] J. Jensen and A. K. Mackintosh, Rare Earth Magnetism (Clarendon, Oxford, 1991).

[27] P. Schlottmann, Theory of Heavy Fermions and Valence Fluctuations (Springer, Berlin, 1985).

[28] N. Read and D. M. News, J. Phys. C **16**, L1055 (1983).

[29] A. C. Hewson and J. W. Rasul, J. Magn. Magn. Mater. **47-48**, 339 (1985).
[30] N. Tsujii, H. Kontani, and K. Yoshimura, Phys. Rev. Lett. **94**, 057201 (2005).
[31] D. L. Cox and N. Grewe, Z. Phys. B **71**, 321 (1988).
[32] F. J. Blatt, P. A. Schroeder, C. L. Foiles, and D. Greig, Thermoelectric Power of Metals (Plenum, New York, 1976).
[33] M. Kohler, Z. Phys. **126**, 481 (1949).
[34] K. Behnia, D. Jaccard, and J. Flouquet, J. Phys. Condens. Matter **16**, 5187 (2004).